INTERNATIONAL JOURNAL OF
NUMERICAL ANALYSIS AND MODELING
Volume 6, Number 3, Pages 402–419

NUMERICAL SOLUTION OF A NON-SMOOTH VARIATIONAL PROBLEM ARISING IN STRESS ANALYSIS : THE SCALAR CASE

ALEXANDRE CABOUSSAT AND ROLAND GLOWINSKI

Abstract. A non-smooth constrained minimization problem arising in the stress analysis of a plastic body is considered. A numerical method for the computation of the load capacity ratio is presented to determine if the elastic body fractures under external traction. In the scalar case, the maximum principle allows one to reduce the problem to a convex one under linear constraints. An augmented Lagrangian method, together with an approximation by finite elements is advocated for the computation of the load capacity ratio and the corresponding elastic stress. The generalized eigenvalues and eigenvectors of the corresponding operator are computed for various two-dimensional bodies and fractures are discussed.

Key Words. Non-smooth optimization, Stresses analysis, Augmented Lagrangian method, Finite elements approximation, Elasticity theory.

1. Introduction and Motivations

The numerical solution of a non-smooth minimization problem arising in the stress analysis of a plastic body is investigated. The problem of interest is the computation of the maximal stress of an elastic three-dimensional body under external forces [3, 18]. The computation of that threshold allows one to determine if the material can support the forces applied to it or if the traction on the material or its boundary is too large.

Consider a homogeneous isotropic elastic body $\Lambda \subset \mathbb{R}^3$. The *load capacity ratio*, as defined in [16], is the maximal positive number C such that the body will not collapse under any external traction field bounded by CY_0, where Y_0 is the elastic limit. It is independent of the distribution of external loading. If we neglect the body forces and consider only forces on the boundary, it implies that no collapse will occur for any field $\mathbf{g}$ on $\partial\Lambda$ as long as ess $\sup_{y\in\partial\Lambda} |\mathbf{g}(y)| < CY_0$. The load capacity ratio is a quantity that depends on the geometry of the domain Λ.

The load capacity ratio is a quantity that also appears in the *limit analysis problem* in Temam (1985) [18], and which represents, from the mechanical standpoint, a criterion to determine if the material can support the imposition of both body and surface external forces.

Load capacity ratio and *stress concentration factors* are used by engineers to compare the maximal stress for a given body with the stress computed analytically for simplified geometries [13, 15]. Such problems also lead to the computation of optimal stresses as in [17, 18].

Received by the editors October 30, 2008 and, in revised form, January 5, 2009.
2000 *Mathematics Subject Classification.* 65K10, 65N30, 49S05, 74G70 .

In this paper, we consider the situation without body forces (see [14, 18] for a theoretical investigation of the addition of body forces). Let us assume that the boundary of Λ is sufficiently smooth and can be decomposed into $\gamma_0 \cup \gamma_1 \cup \gamma_2$, such that $\gamma_i \cap \gamma_j = \emptyset$, $i, j = 0, 1, 2$, $i \neq j$. An external surface traction acts on the boundary γ_1, while the body is fixed on the boundary γ_0.

When the domain Λ is an infinite cylinder oriented along one direction of space and the external surface traction is oriented along that direction, the limit analysis problem can be written as a scalar problem. The numerical approximation of the scalar case is considered here, namely to compute the load capacity ratio when considering a surface traction field oriented along the invariant direction of Λ. Following [1, 2], a numerical method for the approximation of the inverse $\delta := C^{-1}$ of the load capacity ratio is proposed.

Let Ω be the two-dimensional domain obtained by cutting Λ perpendicularly to its invariance direction, and $\Gamma_i = \gamma_i \cap \bar{\Omega}$, $i = 0, 1, 2$. Our aim is therefore to compute the quantity

$$\delta = \inf_{v \in \Sigma} \int_\Omega |\nabla v| \, dx,$$

where $\Sigma = \left\{ v \in V_0, \int_{\Gamma_1} |v| \, dS = 1 \right\}$ and $V_0 = \left\{ v \in H^1(\Omega),\ v = 0,\ \text{on } \Gamma_0 \right\}$.

Such non-smooth optimization problems require appropriate solution methods [1, 4, 9, 10]; they are related to the numerical approximation of the degenerated eigenvalues of non-smooth operators [2, 12]. In this article, an augmented Lagrangian method is advocated and applied to two-dimensional domains, without introducing any regularization or convexification parameters [8, 11, 12] (other than the regularization coming from the space approximation).

In Section 2, the model problem is derived and the scalar problem is justified; the maximum principle is used to transform the problem into a convex optimization problem under linear constraints. Section 3 presents an augmented Lagrangian algorithm for the solution of such non-smooth optimization problems that takes advantage of linearity properties. The finite element discretization is detailed in Section 4. Numerical results in various settings are finally given in Section 5, together with the numerical investigation of fractures when modifying the boundaries under traction and the fixed boundaries.

2. Modeling of Elastic Bodies and the Limit Analysis Problem

Let us consider a elastic material body that occupies a domain $\Lambda \subset \mathbb{R}^3$. The smooth boundary of the domain Λ is partitioned into $\partial\Lambda = \gamma_0 \cup \gamma_1 \cup \gamma_2$ such that $\gamma_i \cap \gamma_j = \emptyset$, $i \neq j$. The elastic material is under body forces $\mathbf{f} \in L^2(\Lambda)^3$ and boundary forces $\mathbf{g} \in L^2(\gamma_1)^3$. The variational problem for the computation of the elastic displacement of the body reads as follows

$$\inf_{\mathbf{v} \in \mathbf{V}_0} \left[\int_\Lambda \psi(\mathbf{D}(\mathbf{v})) dV - L(\mathbf{v}) \right], \tag{1}$$

where $\mathbf{D}(\mathbf{v}) = \dfrac{1}{2} \left(\nabla \mathbf{v} + \nabla \mathbf{v}^T \right)$ is the deformation tensor, $\psi(\cdot)$ is a proper, lower semi-continuous convex function that characterizes the material properties,

$$L(\mathbf{v}) = \int_\Lambda \mathbf{f} \cdot \mathbf{v} dV + \int_{\gamma_1} \mathbf{g} \cdot \mathbf{v} dS,$$

and $\mathbf{V}_0 = \left\{\mathbf{v} \in H^1(\Omega)^3,\ \mathbf{v}|_{\gamma_0} = 0\right\}$. The function $\psi(\cdot)$ can be expressed, for instance, in terms of the Lamé coefficients in linear elasticity models.

Problem (1) has a finite objective value when the elastic body can resist external forces. Following [18], let us introduce an equivalent formulation for (1) to give a criterion for such a situation to happen. The equivalent problem reads as follows:

$$\inf_{\mathbf{v}\in\mathbf{W}_0} \int_\Lambda |\mathbf{D}(\mathbf{v})|\, dV - L(\mathbf{v}), \tag{2}$$

where $\mathbf{W}_0 = \left\{\mathbf{v} \in H^1(\Omega)^3,\ \mathbf{v}|_{\gamma_0} = 0\,,\ \nabla\cdot\mathbf{v} = 0\right\}$, when homogeneous Dirichlet boundary conditions are considered, and by noticing that the infimum is realized on the set of divergence free functions.

The following problem is closely related to (2) and allows one to give a criterion on the finite value of the solution to (1). It can be derived as

$$\inf_{\mathbf{v}\in\tilde{\mathbf{W}}_0} \frac{\int_\Lambda |\mathbf{D}(\mathbf{v})|\, dV}{L(\mathbf{v})}, \tag{3}$$

where $\tilde{\mathbf{W}}_0 = \{\mathbf{v} \in \mathbf{W}_0 \,:\, L(\mathbf{v}) > 0\}$. This particular optimization problem is not convex, but because of the homogeneity of the L^1-norm, it is equivalent to the so-called *limit analysis problem*:

$$\delta := \inf_{\mathbf{v}\in\hat{\mathbf{W}}_0} \int_\Lambda |\mathbf{D}(\mathbf{v})|\, dV, \tag{4}$$

where $\hat{\mathbf{W}}_0 = \left\{\mathbf{v} \in H^1(\Omega)^3,\ \mathbf{v}|_{\gamma_0} = 0\,,\ \nabla\cdot\mathbf{v} = 0,\ L(\mathbf{v}) = 1\right\}$. Problem (4) is a nonsmooth convex optimization problem.

One can show (see *e.g.* [18]) that the infimum of (1) is finite if and only if $\delta \geq 1$ in (4). This result is a strong incentive to be able to compute δ for a given three-dimensional domain Λ, and to determine *a priori* if the elastic body sustains the external forces or if the elastic body fractures (*i.e.* if the displacement $\mathbf{v}$ becomes discontinuous).

In the sequel, let us consider the case without body forces $\mathbf{f} = 0$. By taking the supremum over all possible traction fields $\mathbf{g} \in L^2(\gamma_1)^3$ such that $|\mathbf{g}| \leq 1$, one has $\mathbf{g}\cdot\mathbf{v} = |\mathbf{v}|$ and (4) reads:

$$\inf_{\mathbf{v}\in\mathbf{W}} \int_\Lambda |\mathbf{D}(\mathbf{v})|\, dV, \tag{5}$$

where $\mathbf{W} = \left\{\mathbf{v} \in H^1(\Omega)^3,\ \mathbf{v}|_{\gamma_0} = 0\,,\ \nabla\cdot\mathbf{v} = 0,\ \displaystyle\int_{\gamma_1} |\mathbf{v}|\, dS = 1\right\}$.

Let us consider $\Lambda \subset \mathbb{R}^3$ an infinite cylinder, oriented for instance along the Ox_3 axis. Let us consider traction fields $\mathbf{g} \in L^2(\gamma_1)$, $|\mathbf{g}| \leq 1$ on the boundary γ_1 that are aligned with the Ox_3 axis, as illustrated in Figure 1.

The elastic stress field $\mathbf{v} \in H^1(\Lambda)^3$ can therefore be written as $\mathbf{v}(x_1, x_2, x_3) = (0\,,\,0\,,\,v(x_1,x_2,x_3))^T$. In that case, $|\mathbf{D}(\mathbf{v})| = |\nabla v|$ and $\nabla\cdot\mathbf{v} = \frac{\partial v}{\partial x_3} = 0$ implies $v(x_1,x_2,x_3) = v(x_1,x_2)$. Problem (5) becomes a scalar problem that we detail as follows: let $\Omega \subset \mathbb{R}^2$ be a bounded domain (in the Ox_1x_2-plane) obtained by cutting Λ perpendicularly to Ox_3, with a smooth boundary $\partial\Omega = \Gamma_0 \cup \Gamma_1 \cup \Gamma_2$,

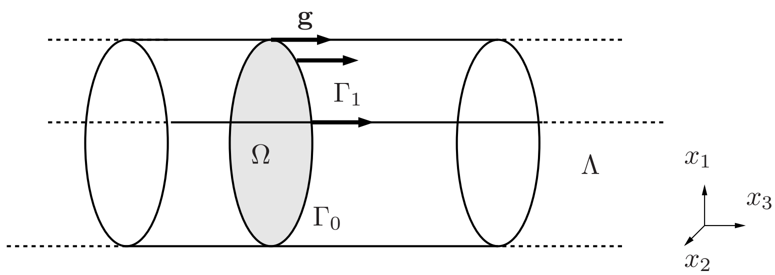

FIGURE 1. Infinite three-dimensional cylinder Λ with cross-section Ω: sketch and notations.

$\Gamma_i = \gamma_i \cap \overline{\Omega}$. Within this framework the solution of (5) corresponds to solving the following non-smooth problem (with $dx = dx_1 dx_2$):

$$\delta := \inf_{v \in \Sigma} \int_\Omega |\nabla v| \, dx, \tag{6}$$

where

$$\begin{aligned} \Sigma &= \left\{ v \in V_0, \int_{\Gamma_1} |v| \, ds = 1 \right\}, \\ V_0 &= \left\{ v \in H^1(\Omega), \, v = 0, \text{ on } \Gamma_0 \right\}. \end{aligned}$$

Note that δ defined by (6) is the inverse of the *load capacity ratio* defined as in [16] ($\delta = 1/C$). If $\delta \geq 1$, the infinite cylinder of cross-section Ω sustain all (normalized) surface traction $\mathbf{g}$. Otherwise, the material presents a fracture. This statement will be confirmed by numerical experiments in Section 5. The objective function and equality constraint in (6) are both non-smooth. However, the infimum has the following property:

Lemma 1. *If $v \in \Sigma$ satisfies the infimum in (6), then $|v|$ also satisfies the same infimum.*

Proof. Clearly, if $v \in \Sigma$, then $|v|$ also belongs to Σ. Moreover

$$\int_\Omega |\nabla |v|| \, dx = \int_\Omega |\nabla v| \, dx,$$

implying that if the infimum is realized for v, it is also realized for $|v|$, and conclusion follows. □

The corollary of this result is that one can actually look for

$$v \in \Sigma^\star = \left\{ v \in V_0, \int_{\Gamma_1} v ds = 1 \, , \, v \geq 0 \right\}$$

and the equality constraint in $\Sigma^\star$ becomes a linear equality constraint, that can be handled with a Lagrange multiplier.

Remark 1. *This transformation is not valid for the vectorial case, when $\mathbf{v} \in H^1(\Omega)^d$, $d = 2, 3$ and $\int_{\Gamma_1} |\mathbf{v}| \, ds = 1$, and the situation is not invariant along Ox_3.*

In the following sections, we present a numerical method based on an augmented Lagrangian algorithm to compute finite element approximations of δ and corresponding functions v satisfying the infimum (6). The computation of these numerical approximations allows one to determine if the elastic stress of an elastic body with cross-section Ω presents a discontinuity under a surface traction.

3. Numerical Algorithm : An Augmented Lagrangian Approach

In the sequel, we address the solution of (6) via an augmented Lagrangian method (keeping in mind the equivalence with alternating direction iteration methods). Let us define $\mathbf{q} = \nabla v \in L^2(\Omega)^2$, $y = v \in L^2_+(\Omega) = \left\{\varphi \in L^2(\Omega) : \varphi \geq 0\right\}$, and $\Sigma_+ = \left\{v \in V_0,\ \int_{\Gamma_1} v ds = 1\right\}$. Problem (6) is equivalent to

$$\delta = \inf_{(v,\mathbf{q},y)\in\mathcal{K}} \int_\Omega |\mathbf{q}|\, dx, \tag{7}$$

where

$$\mathcal{K} = \left\{(v,\mathbf{q},y) \in \Sigma_+ \times L^2(\Omega)^2 \times L^2_+(\Omega) : \nabla v - \mathbf{q} = 0, v - y = 0\right\}.$$

Let r_1, r_2 be two positive parameters and $r = \{r_1, r_2\}$. Let us define the following scalar products

$$\begin{aligned} (\mathbf{p},\mathbf{q}) &:= \int_\Omega \mathbf{p}\cdot\mathbf{q} dx \quad \forall \mathbf{p},\mathbf{q} \in L^2(\Omega)^2 \\ <\varphi,\psi> &:= \int_\Omega \varphi\psi dx \quad \forall \varphi,\psi \in L^2(\Omega) \end{aligned} \tag{8}$$

The augmented Lagrangian method discussed here [9, 10] consists of searching for a *saddle point* of the following augmented Lagrangian functional:

$$\begin{aligned} \mathcal{L}_r(v,\mathbf{q},y;\boldsymbol{\mu}_1,\mu_2) &= \int_\Omega |\mathbf{q}|\, dx + \frac{r_1}{2}\int_\Omega |\nabla v - \mathbf{q}|^2\, dx + (\boldsymbol{\mu}_1, \nabla v - \mathbf{q}) \\ &\quad + \frac{r_2}{2}\int_\Omega |v-y|^2\, dx + <\mu_2, v - y>. \end{aligned} \tag{9}$$

Namely, we are looking for $\{u,\mathbf{p},z,\boldsymbol{\lambda}_1,\lambda_2\} \in \Sigma_+ \times L^2(\Omega)^2 \times L^2_+(\Omega) \times L^2(\Omega)^2 \times L^2(\Omega)$ such that

$$\mathcal{L}_r(u,\mathbf{p},z;\boldsymbol{\mu}_1,\mu_2) \leq \mathcal{L}_r(u,\mathbf{p},z;\boldsymbol{\lambda}_1,\lambda_2) \leq \mathcal{L}_r(v,\mathbf{q},y;\boldsymbol{\lambda}_1,\lambda_2), \tag{10}$$

for all $\{v,\mathbf{q},y,\boldsymbol{\mu}_1,\mu_2\} \in \Sigma \times L^2(\Omega)^2 \times L^2_+(\Omega) \times L^2(\Omega)^2 \times L^2(\Omega)$. Note that the introduction of the auxiliary variables $\mathbf{p} \in L^2(\Omega)^2$ and $z \in L^2_+(\Omega)$ allows one to decouple the constraint on the positiveness of the variable u, the non-smooth term $|\nabla v|$, and the constraint on the boundary Γ_1.

An Uzawa-Douglas-Rachford type algorithm reads as follows:
let $u^{-1} \in V_0$, $\boldsymbol{\lambda}_1^0 \in L^2(\Omega)^2$ and $\lambda_2^0 \in L^2(\Omega)$ be arbitrary given functions. Then, for $n = 0, 1, 2, \ldots$

(a) Solve

$$\mathbf{p}^n = \arg\min_{\mathbf{q}\in L^2(\Omega)^2} \left[\int_\Omega |\mathbf{q}|\, dx + \frac{r_1}{2}\int_\Omega |\mathbf{q}|^2\, dx - (r_1\nabla u^{n-1} + \boldsymbol{\lambda}_1^n, \mathbf{q})\right]. \tag{11}$$

Problem (11) does not involve any derivatives and can be solved pointwise *a.e.* in Ω. It leads to the following closed form solution for $\mathbf{p}^n$ [2, 5, 7]:

$$\mathbf{p}^n(x) = \begin{cases} \dfrac{1}{r_1}\left(1 - \dfrac{1}{|\mathbf{X}^n(x)|}\right)\mathbf{X}^n(x), & \text{if } |\mathbf{X}^n(x)| > 1, \\ 0, & \text{if } |\mathbf{X}^n(x)| \leq 1, \end{cases} \quad , \ a.e.\, x \in \Omega,$$

where $\mathbf{X}^n = r_1 \nabla u^{n-1} + \boldsymbol{\lambda}_1^n \in L^2(\Omega)^2$.

(b) Solve

$$z^n = \arg \min_{z \in L^2_+(\Omega)} \left[\frac{r_2}{2}\int_\Omega |z|^2\, dx - < r_2 u^{n-1} + \lambda_2^n, z >\right]. \tag{12}$$

The first order conditions relative to (12) read: find $z^n \in L^2_+(\Omega)$ such that, for all $w \in L^2(\Omega)$,

$$r_2 < z^n, w > = < r_2 u^{n-1} + \lambda_2^n, w > . \tag{13}$$

This equation consists of an L^2-projection on the set of positive functions in $L^2(\Omega)$ and can also be solved pointwise. The positiveness is ensured pointwise by truncation, so that $z \in L^2_+(\Omega)$. Therefore:

$$z^n(x) = \frac{1}{r_2}\left(r_2 u^{n-1}(x) + \lambda_2^n(x)\right)_+, \quad a.e.\, x \in \Omega. \tag{14}$$

(c) Solve

$$\begin{aligned} u^n = \arg \min_{v \in \Sigma_+} \quad & \left[\frac{r_1}{2}\int_\Omega |\nabla v|^2\, dx + \frac{r_2}{2}\int_\Omega |v|^2\, dx\right. \\ & \left. - < r_2 z^n - \lambda_2^n, v > - (r_1 \mathbf{p}^n - \boldsymbol{\lambda}_1^n, \nabla v)\right]. \end{aligned} \tag{15}$$

The constraint $v \in \Sigma_+$ implies that the solution must satisfy $\displaystyle\int_{\Gamma_1} v ds = 1$. A Lagrange multiplier $\chi \in \mathbb{R}$ is introduced to handle the above scalar equality constraint. The corresponding Lagrangian reads:

$$\begin{aligned} \mathcal{L}(v, \chi) &= \frac{r_1}{2}\int_\Omega |\nabla v|^2\, dx + \frac{r_2}{2}\int_\Omega |v|^2\, dx \\ & - < r_2 z^n - \lambda_2^n, v > - (r_1 \mathbf{p}^n - \boldsymbol{\lambda}_1^n, \nabla v) + \chi\left(\int_{\Gamma_1} v ds - 1\right). \end{aligned} \tag{16}$$

The first order optimality conditions corresponding to (15) (16) read as follows: find $u^n \in \Sigma_+$ and $\chi^n \in \mathbb{R}$ such that, for all $w \in V_0$:

$$\begin{aligned} & r_1(\nabla u^n, \nabla w) + r_2 < u^n, w > = \\ & < r_2 z^n - \lambda_2^n, w > + (r_1 \mathbf{p}^n - \boldsymbol{\lambda}_1^n, \nabla w) + \chi^n \int_{\Gamma_1} w ds. \end{aligned} \tag{17}$$

$$\int_{\Gamma_1} u^n ds = 1. \tag{18}$$

Equation (17) is linear with respect to the multiplier χ^n. It suffices therefore to solve (17) for two values of χ^n, *e.g.* $\chi^n = 0$ and $\chi^n = 1$, with corresponding solutions being u_0^n and u_1^n, and then consider the linear combination that satisfies (18), namely:

$$u^n = (1 - f^n)u_0^n + f^n u_1^n,$$

where

$$f^n = \frac{1 - \displaystyle\int_{\Gamma_1} u_0^n ds}{\displaystyle\int_{\Gamma_1} u_1^n ds - \int_{\Gamma_1} u_0^n ds} \in \mathbb{R},$$

so that the linear combination satisfies $\displaystyle\int_{\Gamma_1} u^n ds = 1$.

(d) Update the multipliers $\boldsymbol{\lambda}_1^n \in L^2(\Omega)^2$ and $\lambda_2^n \in L^2(\Omega)$ as follows:

$$\boldsymbol{\lambda}_1^{n+1} = \boldsymbol{\lambda}_1^n + r_1(\nabla u^n - \mathbf{p}^n), \tag{19}$$

$$\lambda_2^{n+1} = \lambda_2^n + r_2(u^n - z^n), \tag{20}$$

until convergence is reached.

The augmented Lagrangian algorithm produces a sequence of iterates $\{u^n\}_{n\geq 0}$ that eventually converges to the function realizing the infimum of (6).

Let us define $BV(\Omega)$ as the space of functions of bounded variation over Ω. Numerical experiments show that there are situations where the sequence $\{u^n\}_{n\geq 0}$ converge to a limit belonging to $BV(\Omega)\backslash H^1(\Omega)$. However, the sequence $\{u^n\}_{n\geq 0}$ may converge to a limit in a functional space consisting of functions smoother than the generic $BV(\Omega)$ ones (as illustrated in the numerical results when the sequence converge to a limit in V_0). The regularity of the limit depends, among other things, on the boundaries Γ_0 and Γ_1.

4. Finite Element Approximation

Finite element techniques are used for the numerical implementation of algorithm (11)-(20). Let $h > 0$ be a discretization step. A family $\{\Omega_h\}_h$ of polygonal approximations of the domain Ω is introduced such that $\lim_{h\to 0} \Omega_h = \Omega$, together with $\lim_{h\to 0} \Gamma_{0,h} = \Gamma_0$, and $\lim_{h\to 0} \Gamma_{1,h} = \Gamma_1$. Let us consider a triangulation $\mathcal{T}_h$ of the domain Ω_h satisfying the usual compatibility conditions between triangles. Let us denote by N_e the number of elements of $\mathcal{T}_h$, N_n the number of vertices of $\mathcal{T}_h$ in $\Omega_h\backslash\Gamma_{0,h}$, and N_{n_t} the total number of vertices of $\mathcal{T}_h$ in $\overline{\Omega_h}$. Let K denote a generic element (triangle) of $\mathcal{T}_h$.

Let $\mathbb{P}_k$ be the space of polynomials of degree k. The finite element spaces are defined by

$$
\begin{aligned}
V_h^1 &= \left\{ v \in C^0(\overline{\Omega_h}) \,:\, v|_K \in \mathbb{P}_1,\, \forall K \in \mathcal{T}_h \right\}, \\
V_h^0 &= \left\{ \mathbf{q} \in L^2(\Omega_h)^2 \,:\, \mathbf{q}|_K \in \mathbb{P}_0^2,\, \forall K \in \mathcal{T}_h \right\}, \\
V_{0,h}^1 &= \left\{ v \in V_h^1 \,:\, v|_{\Gamma_{0,h}} = 0 \right\}. \\
V_{+,h}^1 &= \left\{ v \in V_h^1 \,:\, v \geq 0 \right\}, \\
\Sigma_{+,h} &= \left\{ v \in V_h^1 \,:\, v|_{\Gamma_{0,h}} = 0,\, \int_{\Gamma_{1,h}} v ds = 1 \right\}.
\end{aligned}
$$

Let φ_j, $j = 1, \ldots, N_n$ and ψ_i, $i = 1, \ldots, N_e$ be the finite element basis functions of $V_{0,h}^1$ and V_h^0 respectively, based on the triangulation $\mathcal{T}_h$. Problem (6) is therefore approximated by

$$
\min_{v_h \in \Sigma_{+,h} \cap V_{+,h}^1} \int_{\Omega_h} |\nabla v_h| \, dx. \tag{21}
$$

Next, we define *discrete* scalar products. Let P_j be any vertex of $\mathcal{T}_h$ and A_j be the area of the polygon which is the union of those triangles of $\mathcal{T}_h$ which have P_j as a common vertex. Then:

$$
\begin{aligned}
(\mathbf{p}_h, \mathbf{q}_h)_{0,h} &= \sum_{K \in \mathcal{T}_h} |K| \, \mathbf{p}_h|_K \cdot \mathbf{q}_h|_K, \quad \forall \mathbf{p}_h, \mathbf{q}_h \in L^2(\Omega)^2 \\
< \varphi_h, \psi_h >_{0,h} &= \frac{1}{3} \sum_{j=1}^{N_n} A_j \varphi(P_j) \psi(P_j), \quad \forall \varphi_h, \psi_h \in L^2(\Omega).
\end{aligned} \tag{22}
$$

The discrete version of algorithm (11)-(20) consists in looking for approximations $u_h \in \Sigma_{+,h}$, $\mathbf{p}_h \in V_h^0$, $z_h \in V_{+,h}^1$, $\boldsymbol{\lambda}_{1,h} \in V_h^0$ and $\lambda_{2,h} \in V_h^1$ of $u, \mathbf{p}, z, \boldsymbol{\lambda}_1$ and λ_2, respectively, that are computed according to the following discretized algorithm. Some subscripts h are omitted in the sequel.

Let $u^{-1} \in \Sigma_{+,h}$ (or $V_{0,h}^1$), $\boldsymbol{\lambda}_1^0 \in V_h^0$ and $\lambda_2^0 \in V_h^1$ be arbitrary given functions. Then, for $n = 0, 1, 2, \ldots$

(a) Solve

$$
\mathbf{p}^n = \arg \min_{\mathbf{q} \in (V_h^0)^2} \int_{\Omega_h} |\mathbf{q}| \, dx + \frac{r_1}{2} \int_{\Omega_h} |\mathbf{q}|^2 \, dx - (\mathbf{X}^n, \mathbf{q})_{0,h},
$$

where $\mathbf{X}^n := r_1 \nabla u^{n-1} + \boldsymbol{\lambda}_1^n$. Locally on each element K, this corresponds to solving

$$
\min_{\mathbf{q}_i \in \mathbb{R}^2} \left[|\mathbf{q}_i| + \frac{r_1}{2} |\mathbf{q}_i|^2 - \mathbf{X}_i^n \cdot \mathbf{q}_i \right], \quad i = 1, \ldots, N_e. \tag{23}
$$

The minimum occurs when $\mathbf{q}_i = \alpha_i \mathbf{X}_i^n$, $\alpha_i \in \mathbb{R}$, $\alpha_i \geq 0$; solving the first order optimality conditions leads to $\alpha_i = \dfrac{1}{r_1} \left(1 - \dfrac{1}{|\mathbf{X}_i^n|} \right)^+$ [6], where

$$
\left(1 - \frac{1}{|\mathbf{X}_i^n|} \right)^+ = \begin{cases} \left(1 - \dfrac{1}{|\mathbf{X}_i^n|} \right), & \text{when } \left(1 - \dfrac{1}{|\mathbf{X}_i^n|} \right) \geq 0, \\ 0, & \text{otherwise.} \end{cases}
$$

Therefore:

$$\mathbf{p}_i^n = \alpha_i \mathbf{X}_i^n = \begin{cases} \dfrac{1}{r_1}\left(1 - \dfrac{1}{|\mathbf{X}_i^n|}\right)\mathbf{X}_i^n, & \text{if } |\mathbf{X}_i^n| > 1, \\ 0, & \text{if } |\mathbf{X}_i^n| \le 1. \end{cases}$$

(b) Solve

$$z^n = \arg \min_{z \in V^1_{+,h}} \left[\frac{r_2}{2} \int_\Omega |z|^2 \, dx - < r_2 u^{n-1} + \lambda_2^n, z >_{0,h} \right]. \tag{24}$$

The first order conditions can be written as: find $z^n \in V^1_{+,h}$ such that

$$r_1 < z^n, w >_{0,h} = < r_2 u^{n-1} + \lambda_2^n, w >_{0,h}, \quad \forall w \in V^1_{0,h}.$$

In order to take into account the positiveness constraint, the solution is truncated pointwise in order to give:

$$z^n(P_i) = \frac{1}{r_1}\left(r_2 u^{n-1}(P_i) + \lambda_2^n(P_i)\right)_+, \quad i = 1, \ldots, N_{n_t}. \tag{25}$$

(c) Compute $u^n \in \Sigma_{+,h}$, $\chi^n \in \mathbb{R}$, satisfying, for all $w \in V^1_{0h}$:

$$\begin{aligned} & r_1(\nabla u^n, \nabla w)_{0,h} + r_2 < u^n, w >_{0,h} = \\ & < r_2 z^n - \lambda_2^n, w >_{0,h} + (r_1 \mathbf{p}^n - \boldsymbol{\lambda}_1^n, \nabla w)_{0,h} + \chi^n \int_{\Gamma_{1,h}} w ds, \end{aligned} \tag{26}$$

together with $\int_{\Gamma_{1,h}} u^n ds = 1$. By linearity, (26) is solved for $\chi^n = 0$ and $\chi^n = 1$ to obtain the respective solutions u_0^n and u_1^n. Then we set, for $i = 1, \ldots, N_n$:

$$\begin{aligned} u^n(P_i) &= (1 - f_h^n) u_0^n(P_i) + f_h^n u_1^n(P_i), \quad \text{where} \\ f_h^n &= \frac{1 - \int_{\Gamma_{1,h}} u_0^n ds}{\int_{\Gamma_{1,h}} u_1^n ds - \int_{\Gamma_{1,h}} u_0^n ds}. \end{aligned}$$

The boundary integrals on Γ_1 are approximated by numerical quadrature (trapezoidal formula). By setting $u^n = \sum_{j=1}^{N_n} u_j \varphi_j$, (26) reads, for χ^n given,

$$\begin{aligned} & \sum_{j=1}^{N_n} u_j \left(r_1 (\nabla \varphi_j, \nabla \varphi_i)_{0,h} + r_2 < \varphi_j, \varphi_i >_{0,h} \right) = \\ & < r_2 z^n - \lambda_2^n, \varphi_i >_{0,h} + (r_1 \mathbf{p}^n - \boldsymbol{\lambda}_1^n, \nabla \varphi_i)_{0,h} + \chi^n \int_{\Gamma_{1,h}} \varphi_i ds, \quad i = 1, \ldots, N_n. \end{aligned}$$

This corresponds to the solution of a linear system $A\vec{u} = \vec{b}$, with $\vec{u} = (u_i)_{i=1}^{N_n}$, $\vec{b} = (b_i)_{i=1}^{N_n}$ and $A = (A_{ij})_{i,j=1}^{N_n}$ defined by

$$\begin{aligned} A_{ij} &= r_1 (\nabla \varphi_j, \nabla \varphi_i)_{0,h} + r_2 < \varphi_j, \varphi_i >_{0,h}, \\ b_i &= < r_2 z^n - \lambda_2^n, \varphi_i >_{0,h} + (r_1 \mathbf{p}^n - \boldsymbol{\lambda}_1^n, \nabla \varphi_i)_{0,h} + \chi^n \int_{\Gamma_{1,h}} \varphi_i ds. \end{aligned}$$

(d) Update the multipliers $\boldsymbol{\lambda}_1^n \in (V_h^0)^2$ and $\lambda_2^n \in (V_h^1)$:

$$\boldsymbol{\lambda}_1^{n+1}\big|_K = \boldsymbol{\lambda}_1^n|_K + r_1(\nabla u^n|_K - \mathbf{p}^n|_K), \quad \forall K \in \mathcal{T}_h, \tag{27}$$

$$\lambda_2^{n+1}(P_j) = \lambda_2^n(P_j) + r_2(u^n(P_j) - z^n(P_j)), \quad \forall j = 1, \dots N_{n_t}, \tag{28}$$

until convergence is reached.

5. Numerical Results

Numerical results are presented for various geometries, first to validate the proposed approach and then to discuss the regularity of the solution for large traction. The position of the boundaries Γ_0 and Γ_1 is discussed. Convergence of the finite element approximation when the space parameter h tends to zero is investigated.

5.1. A Linear Problem. A model problem is considered first to validate the proposed algorithm. Consider $\Omega = (0,1) \times (0,1)$, $\Gamma_0 = \{(0, x_2) \ : \ x_2 \in (0,1)\}$, and $\Gamma_1 = \{(1, x_2) \ : \ x_2 \in (0,1)\}$. The problem has linear characteristics since no transverse gradients is created in the Ox_2 direction, and one can show that the minimizer of (6) is given by $v(x_1, x_2) = x_1$, with corresponding value $\delta = 1$. Figure 2 illustrates the eigenfunction u solution of (6). The corresponding eigenvalue δ_h corresponds to the maximal load and is given by $\delta_h = 1$, which implies that the elastic body resists external surface forces. One can verify that no transverse gradient are created by the numerical approximation, and that the solution is therefore invariant along Ox_2. Finer meshes also give the exact value $\delta_h = \delta = 1$.

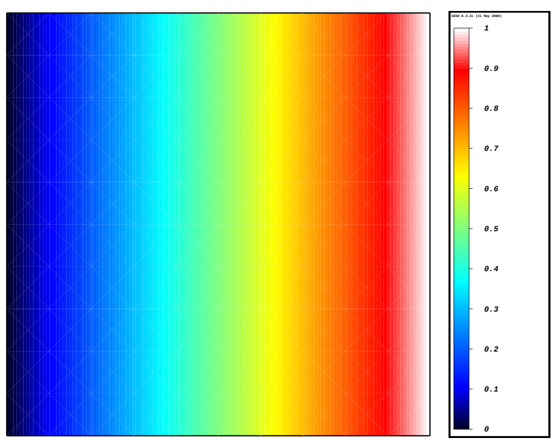

FIGURE 2. Computation of load in a square domain $\Omega = (0,1) \times (0,1)$. Linear case when $\Gamma_0 = \{(0, y) \ : \ y \in (0,1)\}$, and $\Gamma_1 = \{(1, y) \ : \ y \in (0,1)\}$.

5.2. Load Capacity in Bars. Let us consider the domain consisting of the horizontal bar $\Omega = (0,5) \times (0,1)$. Let $a \in (0,5)$ be a variable parameter. Two cases are considered for the boundary conditions:

(a) The traction is forced at the extreme right part of the bar. The boundary where the body is supported is not the complement of the boundary where the traction is imposed, and there exists $\Gamma_2 \subset \partial\Omega$ without load, or essential boundary conditions:

$$\begin{aligned}\Gamma_0 &= \{(0,x_2)\ :\ x_2 \in (0,1)\} \cup \{(x_1,0)\ :\ x_1 \in (0,a)\} \cup \{(x_1,1)\ :\ x_1 \in (0,a)\},\\ \Gamma_1 &= \{(5,x_2)\ :\ x_2 \in (0,1)\},\\ \Gamma_2 &= \partial\Omega \backslash (\Gamma_0 \cup \Gamma_1).\end{aligned}$$

(b) The traction is also forced at the extreme right part of the bar. The boundary where the body is supported is the complement of the boundary where the traction is imposed:

$$\begin{aligned}\Gamma_0 &= \{(0,x_2)\ :\ x_2 \in (0,1)\} \cup \{(x_1,0)\ :\ x_1 \in (0,a)\} \cup \{(x_1,1)\ :\ x_1 \in (0,a)\},\\ \Gamma_1 &= \partial\Omega \backslash \Gamma_0,\\ \Gamma_2 &= \emptyset.\end{aligned}$$

In both cases, the symmetry of the boundary conditions is respected and the solution is symmetric with respect to the axis $x_2 = 0.5$.

Let us consider the case **(a)** first and vary the parameter a from 0 to 5. As a increases, a constant traction is conserved on the extreme right end of the domain Γ_1. The boundary Γ_1 remains identical, but Dirichlet conditions are imposed on a larger part of the boundary. The case **(a)** is illustrated in Figure 3, for various values of the parameter a. As in Figure 2, the solution does not contain any transverse gradients in the Ox_2 direction. The solution u satisfying the minimum in (21) is equal to zero in the subdomain $(0,a) \times (0,1)$ and is linear between $x_1 = a$ and $x_1 = 5$.

The case **(b)** is illustrated in Figure 4. As a increases, the size of the boundary Γ_1 decreases and the corresponding traction is concentrated onto a smaller portion of the boundary. The symmetry is preserved. The solution u satisfying the minimum (21) is therefore equal to zero in the subdomain $(0,a) \times (0,1)$, is constant in the subdomain $(a,5) \times (0,1)$, and jumps on a vertical interface. The material fractures for each value of the parameter a.

Comparing Figures 3 and 4 leads to the following conclusions: when $\Gamma_0 \cup \Gamma_1 \neq \partial\Omega$, the solution u belongs to $H^1(\Omega)$, due to the part of the boundary Γ_2 that does not contain any constraint. The eigenfunction solution of (6) relative to the minimal eigenvalue therefore belongs to $H^1(\Omega)$. When there is no such boundary Γ_2 to allow the "evacuation" of the load, the minimizing sequence produced by the augmented Lagrangian algorithm converges to a limit that is in $BV(\Omega)\backslash H^1(\Omega)$, the space of functions with bounded total variation on Ω, and the total stress presents a jump along the vertical line. The eigenfunction solution of (6) relative to the minimal eigenvalue therefore belongs only to $BV(\Omega)\backslash H^1(\Omega)$.

The numerical approximation of the *load capacity ratio* (or more precisely its inverse) for various values of the parameter a is illustrated in Table 1. The load capacity ratio corresponds to the infimum of the objective function appearing in the limit analysis problem in [18].

TABLE 1. Value of the objective function δ_h vs. Γ_0. First row: case **(a)** with free boundary Γ_2; Second row: case **(b)** with $\Gamma_0 \cup \Gamma_1 = \partial\Omega$.

a	0	1	2	3	4	5
δ_h **(a)**	1	1	1	1	1	1
δ_h **(b)**	0.09259	0.11111	0.14286	0.20000	0.33333	1.0000

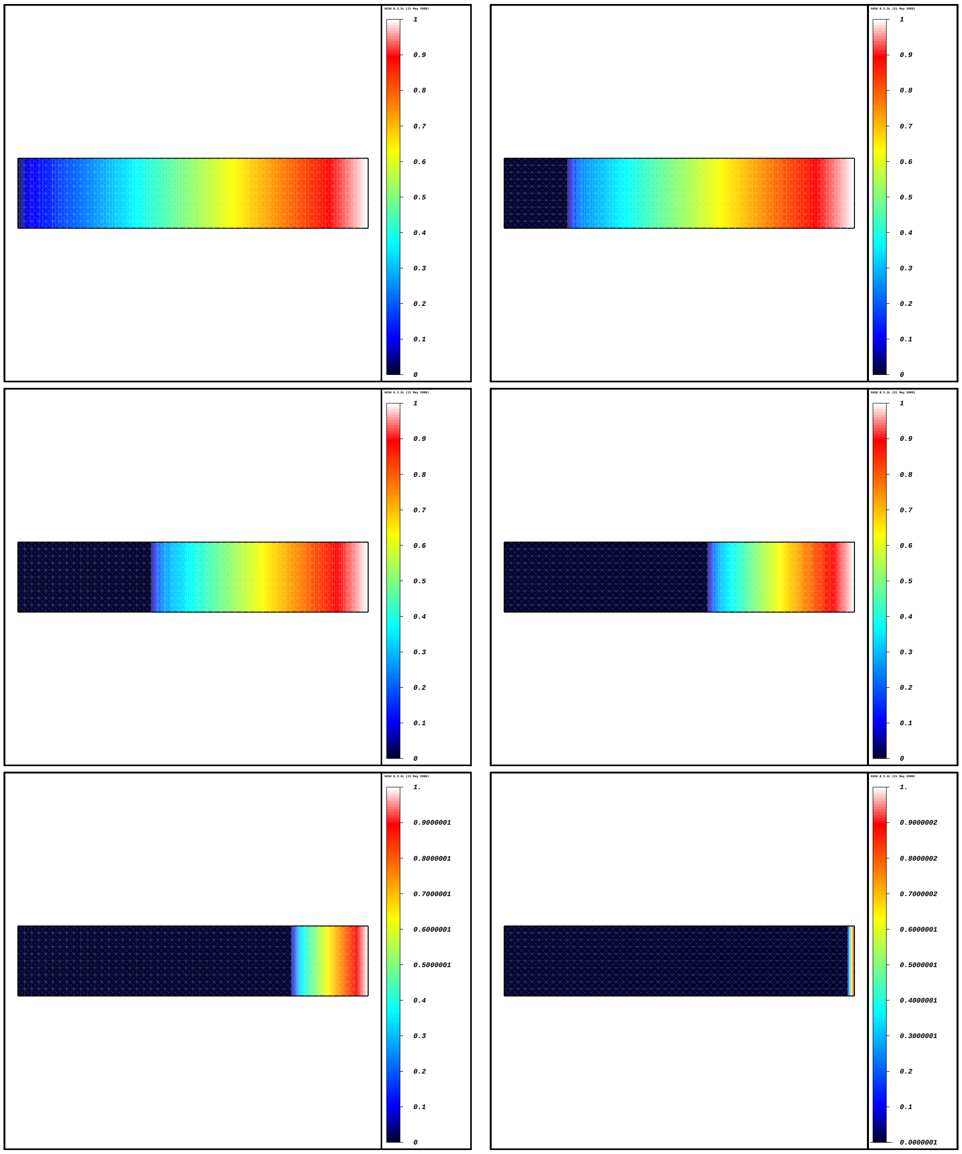

FIGURE 3. Elastic stress for various definitions of the boundary Γ_0. The case when $\Gamma_0 \cup \Gamma_1 \neq \partial\Omega$: $\Gamma_1 = \{(5, x_2) \ : \ x_2 \in (0,1)\}$ and $\Gamma_0 = \{(0, x_2) \ : \ x_2 \in (0,1)\} \cup \{(x_1, 0) \ : \ x_1 \in (0,a)\} \cup \{(x_1, 1) \ : \ x_1 \in (0,a)\}$, for $a = 0, 1, 2, 3, 4, 5$ (left to right, top to bottom). The solution is continuous, piecewise linear, and belongs to $H^1(\Omega)$.

Table 1 allows one to conclude that, when a part of the boundary Γ_2 is let to be free and Γ_1 is constant, the load capacity ratio is invariant with the choice of the fixed Dirichlet boundary, and depends only on the part of the boundary Γ_1 where the traction is enforced. Moreover, since $\delta_h = 1$, the elastic body material resists the external surface traction and there is no discontinuity of the elastic displacement. On the other hand, when $\Gamma_0 \cup \Gamma_1 = \partial\Omega$, increasing Γ_0 (which corresponds to concentrating the same traction on a smaller part of the boundary Γ_1), leads to a

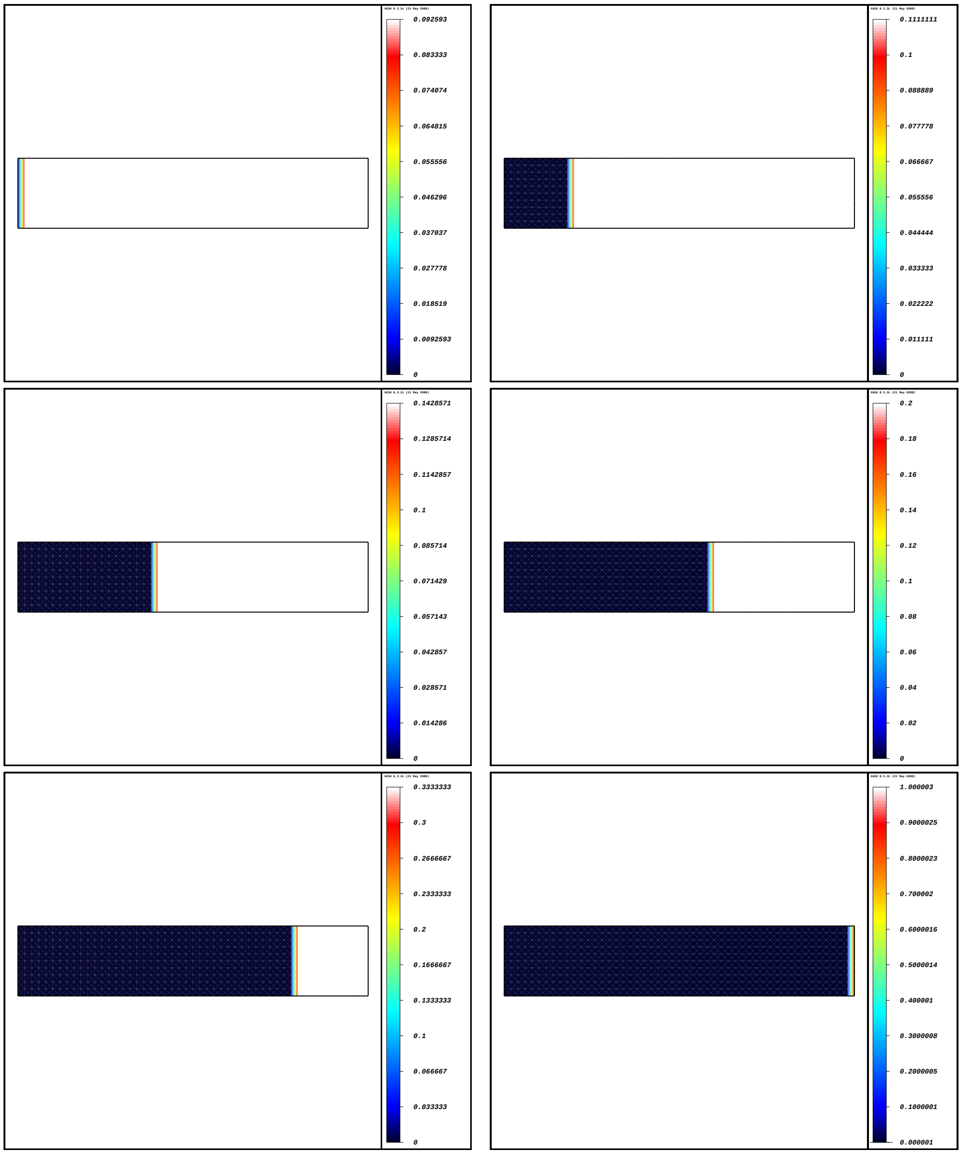

FIGURE 4. Elastic stress for various definitions of the boundary Γ_0. The case when $\Gamma_0 \cup \Gamma_1 = \partial\Omega$: $\Gamma_0 = \{(0, x_2) \ : \ x_2 \in (0,1)\} \cup \{(x_1, 0) \ : \ x_1 \in (0, a)\} \cup \{(x_1, 1) \ : \ x_1 \in (0, a)\}$, for $a = 0, 1, 2, 3, 4, 5$ (left to right, top to bottom) and $\Gamma_1 = \partial\Omega \backslash \Gamma_0$. The solution is piecewise constant, and belongs to $BV(\Omega) \backslash H^1(\Omega)$.

decrease of the load capacity ratio δ_h. The value of the eigenvalue δ_h is 1 when Γ_1 is minimal, and the material resists the traction; then $\delta_h < 1$ and a fracture occurs in the elastic body. In the sequel, we concentrate on the case $\Gamma_2 = \emptyset$, since it results in the convergence of the minimizing sequence to a solution in $BV(\Omega) \backslash H^1(\Omega)$ with less regularity.

5.3. Symmetry Breaking and Fractures. Results exhibited in the previous section have shown that imposing $\Gamma_0 \cup \Gamma_1 = \partial\Omega$ leads to a solution u in $BV(\Omega)$. The case considered here is the unit disk of radius one centered at the origin.

Figure 5 shows the limit solution u for various choices of boundary conditions. Typically Γ_0 is chosen to be a set of segments or points on the boundary. Results show that the solution of (6) is still a function in $BV(\Omega)\backslash H^1(\Omega)$ that presents line and/or point discontinuities induced by the Dirichlet boundary conditions. The line discontinuities are approximated by piecewise linear functions due to the finite element approximation. The point discontinuities are approximated by discrete Dirac measures. Note that, if Γ_0 consists only of a finite set of points, the eigenfunction (*i.e.* the limit of the minimizing sequence) is in $H^1(\Omega)$ and is still regular (imposing pointwise Dirichlet boundary conditions does not create line discontinuities). In all cases $\delta < 1$, which confirms the fracture of the elastic body.

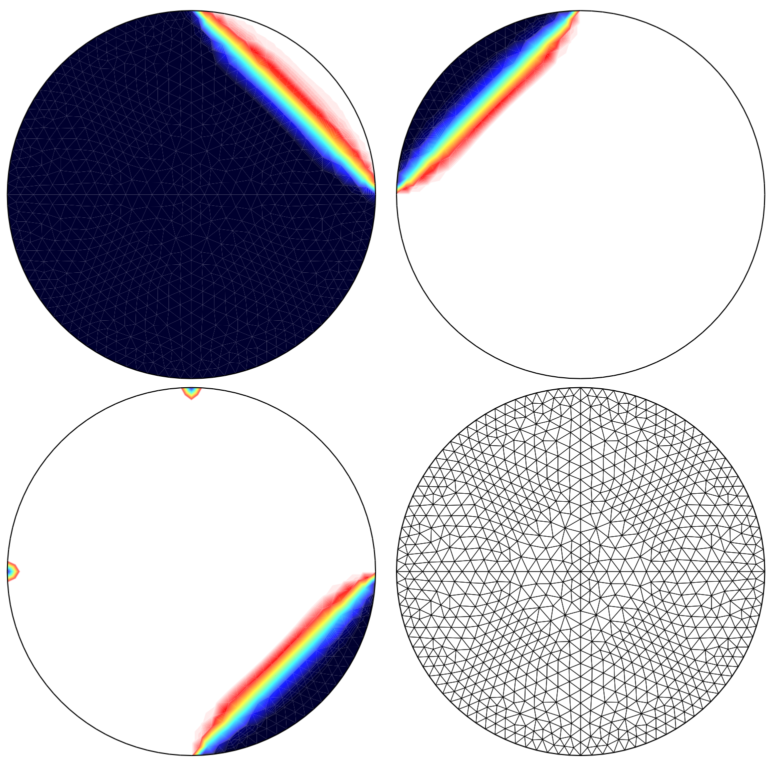

FIGURE 5. Approximation of the elastic stress $u \in BV(\Omega)\backslash H^1(\Omega)$ for various sets of boundary conditions on Ω the unit disc satisfying $\Gamma_0 \cup \Gamma_1 = \partial\Omega$: $\Gamma_0 = \big\{(x_1,x_2) : x_1^2 + x_2^2 = 1, x_1 \geq 0, x_2 \geq 0\big\}$ $\delta_h = 0.920075968$ (top left); $\Gamma_0 = \big\{(x_1,x_2) : x_1^2 + x_2^2 = 1, x_1 \leq 0, x_2 \geq 0\big\}$ $\delta_h = 0.295571999$ (top right); $\Gamma_0 = \big\{(x_1,x_2) : x_1^2 + x_2^2 = 1, x_1 \geq 0, x_2 \leq 0\big\} \cup \{(0,1)\} \cup \{(-1,0)\}$ $\delta_h = 0.354174083$ (bottom left); Triangulation $\mathcal{T}_h$ (bottom right). The boundary conditions create point and line discontinuities.

5.4. Convergence Analysis. Let us consider the case of the horizontal bar $\Omega = (0,5) \times (0,1)$. In order to avoid any mesh effects, let us consider the case $\Gamma_0 =$

$\{(0, x_2) \ : \ x_2 \in (0,1)\} \cup \{(x_1, 0) \ : \ x_1 \in (0,a)\} \cup \{(x_1, 1) \ : \ x_1 \in (0,b)\}$, with $a = 2$ and $b = 3$, and $\Gamma_1 = \partial\Omega \backslash \Gamma_0$ (*i.e.* diagonal cut of the bar), as illustrated in Figure 6 (top line). In that case, the discontinuity line is not aligned with the mesh and mesh effects are avoided. The solution minimizer of (6) belongs to $BV(\Omega) \backslash H^1(\Omega)$.

Figure 6 illustrates the level lines of the approximated eigenfunction that minimizes (6) when the mesh size decreases. As expected, the limit does belong to $BV(\Omega) \backslash H^1(\Omega)$ and a discontinuity occurs along a line, creating a line discontinuity. However, the fracture does not occur along the separation line between Γ_0 and Γ_1, but along a line with a smaller angle: when applying such boundary conditions, the traction imposed by the boundary conditions cannot be sustained and the fracture occurs with a smaller angle. Table 2 shows the values of the approximation δ_h of the eigenvalue δ. As expected, the sequence is decreasing as h decreases.

Since the values in Table 2 are aligned, a least squares method is used to extrapolate a *theoretical* value of $\delta \simeq 0.19637413$ for the limit value $h = 0$. This extrapolated value is used to obtain convergence orders. Figure 7 shows the error plot on a log-log scale of the error $|\delta_h - \delta|$. One can observe a convergence of order one for the finite element approximation of the load capacity ratio.

TABLE 2. Convergence analysis of the approximation of the load capacity ratio for the case of an horizontal bar with diagonal fracture.

h	0.10	0.05	0.025	0.0166
δ_h	0.210653697	0.203507772	0.199944976	0.198746035

Remark 2. *When the discontinuity occurs along a vertical interface as in Figure 4, the approximation of the eigenpairs is much more accurate, since the discontinuity occurs along the mesh direction, and convergence orders are not meaningful.*

6. Conclusions

A non-smooth optimization problem arising in stress analysis and modeling of elastic materials has been investigated. The first generalized eigenvalue of the operator corresponds to the load capacity ratio. The value of that eigenvalue determines if an elastic body with a given geometry resists external surface traction.

The non-smooth problem has been written as a convex problem under linear constraint by using the maximum principle. An augmented Lagrangian method, together with piecewise linear finite elements, has been presented. The influence of boundary conditions on the regularity of the elastic displacement has been investigated, and the formation of fractures has been exhibited. Convergence orders have been obtained for the approximation of the first generalized eigenvalue.

Future work will include the design of numerical methods for the investigation of vectorial problems arising when the traction is perpendicular to the invariance direction of the infinite cylinder.

Acknowledgments

The authors would like to thank Professor R. Segev (Ben Gurion University of the Negev, Israël) for suggesting the investigation of this problem and A. Leonard for her helpful comments. This research was partially supported by the National Science Foundation Grant NSF DMS-0412267.

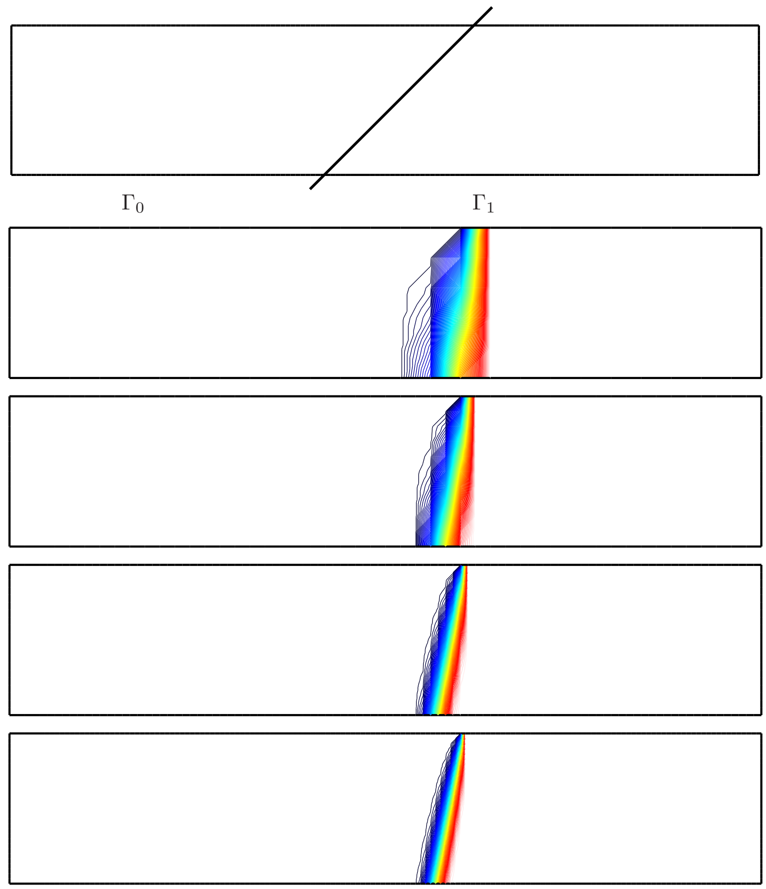

FIGURE 6. Computation of the elastic stress in an horizontal bar with diagonal fracture and convergence of the approximation of the load capacity ratio. Definition of boundary conditions (top picture) Representation of the level lines of the eigenfunction for $h = 0.10$, $h = 0.05$, $h = 0.025$, and $h = 0.0166$ (second to bottom pictures).

References

[1] A. Caboussat and R. Glowinski. A numerical method for a non-smooth advection-diffusion problem arising in sand mechanics. *Com. Pure. Appl. Anal*, 8(1), 2009.

[2] A. Caboussat, R. Glowinski, and V. Pons. An augmented Lagrangian approach to the numerical solution of a non-smooth eigenvalue problem. *SIAM J. Sci. Comp*, submitted, 2008.

[3] P. G. Ciarlet. *Mathematical Elasticity I. Three-Dimensional Elasticity.* Number 20 in Studies in Mathematics and its Applications. North-Holland, 1988.

[4] E. J. Dean and R. Glowinski. Numerical solution of the two-dimensional elliptic Monge-Ampère equation with Dirichlet boundary conditions: an augmented Lagrangian approach. *C. R. Acad. Sci. Paris, Sér. I*, 336:779–784, 2003.

[5] E. J. Dean and R. Glowinski. An augmented Lagrangian approach to the numerical solution of the Dirichlet problem for the elliptic Monge-Ampère equation in two dimensions. *Electronic Transactions in Numerical Analysis*, 22:71–96, 2006.

[6] E. J. Dean and R. Glowinski. Numerical methods for fully nonlinear elliptic equations of the Monge-Ampère type. *Comp. Meth. Appl. Mech. Engrg.*, 195:1344–1386, 2006.

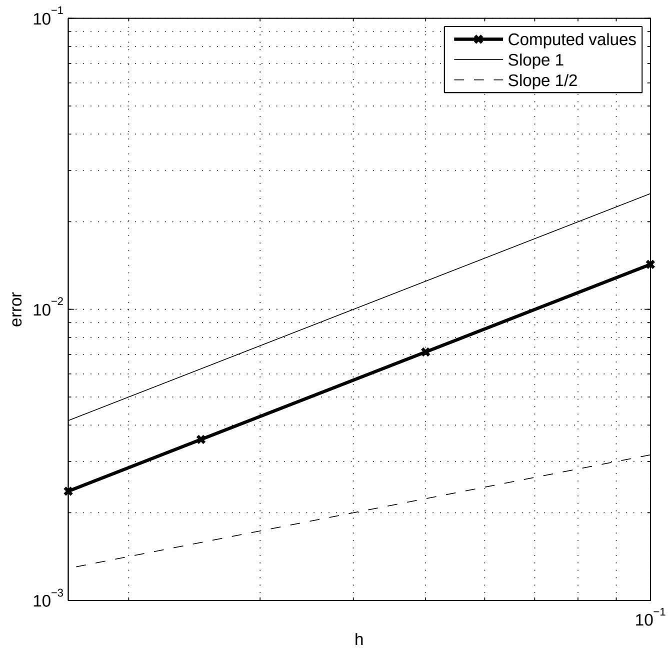

FIGURE 7. Convergence order for the error $e = |\delta_h - \delta|$ for the case of an horizontal bar with diagonal fracture, where $\delta \simeq 0.19637413$ is given by a least-squares extrapolation for $h = 0$ of the computed values obtained in Table 2.

[7] E. J. Dean, R. Glowinski, and G. Guidoboni. On the numerical simulation of Bingham visco-plastic flow: old and new results. *Journal of Non Newtonian Fluid Mechanics*, 142:36–62, 2007.

[8] X. Feng, M. Neilan, and A. Prohl. Error analysis of finite element approximations of the inverse mean curvature flow arising from the general relativity. *Numer. Math.*, 108:93–119, 2007.

[9] R. Glowinski, J.-L. Lions, and R. Trémolières. *Numerical Analysis of Variational Inequalities*. North Holland, 1981.

[10] R. Glowinski and P. Le Tallec. *Augmented Lagrangians and Operator-Splitting Methods in Nonlinear Mechanics*. SIAM, Philadelphia, 1989.

[11] T. Kärkkäinen, K. Kunisch, and K. Majava. Denoising of smooth images using L^1-fitting. *Computing*, 74(4):353–376, 2005.

[12] K. Majava, R. Glowinski, and T. Kärkkäinen. Solving a non-smooth eigenvalue problem using operator-splitting methods. *International Journal of Computer Mathematics*, 84(6):825–846, 2007.

[13] R. Peretz and R. Segev. Bounds on the trace mapping of LD-fields. *Comp. Math. Appl.*, 53(3-4):665–684, 2007.

[14] R. Segev. Generalized stress concentration factors for equilibrated forces and stresses. *J. Elasticity*, 81(3):293–315, 2005.

[15] R. Segev. Generalized stress concentration factors. *Mathematics and Mechanics of Solids*, 11(5):479–493, 2006.

[16] R. Segev. Load capacity of bodies. *Int. J. Nonlinear Mech.*, 42:250–257, 2007.

[17] R. Segev and G. Debotton. Optimal stresses in structures. *preprint*, 2008.

[18] R. Temam. *Mathematical Problems in Plasticity*. Gauthier-Villars, Paris, 1985.

Department of Mathematics, University of Houston, 4800 Calhoun Rd, Houston, TX 77204-3008, USA

E-mail: caboussat@math.uh.edu and roland@math.uh.edu

URL: http://www.math.uh.edu/∼caboussat/ and http://www.math.uh.edu/∼roland/